MTG-IRS LEVEL 2 DATA ASSIMILATION INTO THE ECMWF MODEL

Contract No. EUM/CO/15/4600001613/TA

Kirsti Salonen and Anthony McNally

ECMWF, Shinfield Park, Reading, RG2 9AX, UK

January 2020

Executive summary

The European Centre for Medium-Range Weather Forecasts (ECMWF) has been contracted by the European Organization for the Exploitation of Meteorological Satellites (EUMETSAT) to perform an evaluation of operational Infrared Atmospheric Sounding Interferometer (IASI) retrievals which will be the baseline also for Meteosat Third Generation Infrared Sounder (MTG-IRS) retrievals. The all-sky retrieval function from the operational IASI Level 2 processor in the infrared-only mode has been used in this study. This report presents the main results of the work done during January 2018-December 2019 of the contract (Project Ref. EUM/CO/15/4600001613/TA).

The quality and characteristics of the retrievals have been evaluated by comparing the observatios to their model counterparts. These so called observation minus background (OmB) statistics allow estimation of systematic and random errors and together with the quality information accompanying the retrievals, various investigations can be performed. The results indicate that the overall quality of the retrievals is good as long as strict quality indicators are applied to exclude cloudy scenes for temperature retrievals. Generally the clear sky OmB standard deviations are comparable or slightly larger in magnitude to similar statistics computed for radiosondes. However, due to the vertical resolution of the hyperspectral sounding instrument, the retrievals are rather smooth and often missing fine vertical structures such as low level temperature inversions or detailed structure of the tropopause.

Careful specification of observation errors is an essential step for successful assimilation of any observation type. The assigned observation errors together with the specified background errors determine how much weight is given to the observations in the assimilation system. Observation errors and error correlations for the retrievals have been diagnosed following similar approach than what is used for the operationally used IASI radiances. Investigations reveal that the observation errors are highly correlated between vertical levels and it is essential to take these correlations into account in data assimilation experiments. The error correlations are also scene and location dependent and become increasingly stronger for cloud affected profiles. A scene dependent observation error model and error correlation model have been developed for the cloud affected humidity retrievals to be used in assimilation experiments. Assimilation experiments with the temperature retrievals was restricted to clear sky situations only at this stage.

Assimilation experiments indicate that in clear sky conditions the humidity retrievals have a positive impact on analyses and forecast quality, roughly comparable in magnitude to that obtained when IASI radiances are assimilated. Assimilation of cloud affected humidity retrievals brings further improvements to model analyses and forecasts. Impact can be enhanced by using scene dependent observation errors and error correlations. Currently assimilation of the temperature retrievals degrades the model analyses and forecasts. This is likely due to assimilation of the smooth or missing vertical structures for temperature without taking the limited vertical resolution of the retrievals properly into account.

Contents

1 Introduction

In early days of satellite measurements the information was used in numerical weather prediction (NWP) models as temperature and humidity retrievals. The impact of assimilating the retrievals was from neutral to slightly positive [e.g. Atkins and Jones, 1975, Kelly et al., 1978, Ohring, 1979]. The main benefits were obtained in the southern hemisphere where the conventional observation network was sparse. The NWP systems advanced significantly and by the late 1980s the impact of assimilation of satellite retrievals was often documented to be negative or very variable from case to case [e.g. Kelly and Pailleux, 1988, Andersson et al., 1991, Kelly et al., 1991]. Reason for this was that the short-range forecasts had become more accurate and assimilation of observations in a suboptimal way degraded the analysis and forecasts [Eyre, 2007]. Introduction of variational data assimilation methods enabled the direct use of satellite radiances in the NWP systems and assimilation of radiances is currently the main approach to exploit satellite data in most of the NWP centres with significant improvements in the analysis and forecasts [e.g. Bouttier and Kelly, 2001, McNally et al., 2012, Lord et al., 2016].

Quality of the state of the art retrievals has improved significantly in the past years. Thus, it is interesting to explore what is the impact of retrievals in a current state of the art assimilation system. European Organisation for the Exploitation of Meteorological Satellites (EUMETSAT) is producing forecast independent infrared only statistical retrievals of atmospheric temperature, specific humidity and ozone together with surface temperature, pressure and emissivity from Infrared Atmospheric Sounding Interferometer (IASI) radiances in preparation for future product generation from Infrared Atmospheric Sounding Interferometer (MTG-IRS). The retrievals are produced in all sky conditions. The potential and practical aspects of assimilating the IASI temperature and humidity retrievals has been investigated in the European Centre for Medium-Range Weather Forecasts (ECMWF) system. First, the main focus is on the best of the best clear sky retrievals and the impact is compared to the impact from direct IASI radiance assimilation to get a realistic understanding of the potential of the retrieval assimilation. In the follow on investigations the scene dependence of the observation errors and error correlations are considered and the potential of cloud affected humidity retrievals is assessed.

The report is organised as following. Section 2 summarises the key elements of the EUMETSAT statistical retrieval processing and section 3 discusses shortly the technical aspects of introducing the retrievals into the ECMWF system. Section covers the quality and typical characteristics of the retrievals. Estimating realistic observation errors and error correlations is essential for successful assimilation and section 5 summarises the work done to estimate the retrieval errors and correlations in clear sky situations in the ECMWF system. Section 6 discusses the quality and screening decisions and shows results from assimilation experiments with clear sky retrievals in depleted and in full observing system. Section 7 extends the experimentation to cloud affected retrievals and considers the scene dependence of the observation errors and error correlations. Section 8 discusses the possibility of EUMETSAT importing explicit situation dependent observation errors for the retrievals. Finally, section 9 concludes the findings of the study with a short outlook to the future work.

2 IASI level 2 retrievals

The EUMETSAT level 2 (L2) retrieval processing for IASI will be the baseline for the future L2 product generation of MTG-IRS. The all-sky retrieval function from the operational IASI L2 Product Processing Facility (PPF) version 6 in the infrared only mode has been used to generate the retrievals used in this study. Statistical retrieval methods model the statistical relationship between the observations and the parameters to be retrieved based on a large representative dataset. The linear model is obtained in a so-called training, by regression between the predictors and the target geophysical parameters. The used retrieval method is based on piecewise linear regression (PWLR). More details of the retrieval processing can be found from [e.g. Hultberg and August, 20??, EUMETSAT, 2017] (I found these references online, no information about year/conference for Hultberg and August). For the L2 retrievals considered in this study, the training data set has been constructed from ERA5 reanalysis fields.

The retrievals are complemeted with meta data including geolocation, viewing and solar angles as well as with cloud and quality information. The cloud information is based on observation minus calc (OmC) values. It compares the observed window channel brightness temperature with the corresponding brightness temperature calculated with a radiative transfer model making a clear sky assumption. In addition to the cloud information, quality indicators estimating the uncertainty of the temperature, humidity and ozone retrievals are provided. As infrared radiances are not sensitive to the atmosphere below clouds there is a high degree of correlation between the cloudiness and the quality indicators.

The data is provided in hdf5 format. The atmospheric profiles are provided on 137 ECMWF vertical model levels and surface. In this study the surface variables are not considered.

3 Introducing the retrievals into the ECMWF system

ECMWF develops and operates a global numerical weather prediction system called the integrated forecasting system (IFS). IFS consists of several components: an atmospheric general circulation model, an ocean wave model, a land surface model, an ocean general circulation model and perturbation models for the data assimilation and generation of forecast ensembles. The data assimilation method in use is 4-dimensional variational data assimilation (4D-Var). As part of this study, the IFS system CY45R1 (documentation available at: https://www.ecmwf.int/en/publications/ifs-documentation) has been specially adapted to handle the IASI temperature and humidity retrievals.

The observation input into IFS system is Observational Data Base (ODB) format. A module to create ODB files with the selected content from the hdf5 files has been developed. Each ODB file contains observations for a 12-hour assimilation window used in IFS, including all the meta data provided with the retrievals. Thus, the meta data can be used in validation and quality control when required. To limit the data amount, a pre-screening step to select randomly one out of four profiles is applied, resulting to ∼14 G ODB file / 12-hour assimilation window including both Metop-A and Metop-B IASI retrievals. Similar pre-screening is applied to operationally used IASI radiances, though the warmest field of view is selected for the radiances. For comparison, an ODB file for IASI radiances is quite similar in size than for the retrievals. Overall, ODB files fore IASI radiances are the largest of any observation type currently operationally used in the IFS system.

To produce model counterpart for the temperature and humidity retrievals, observation operators are applied to interpolate the model temperature and specific humidity profiles to the observation locations in horizontal and in vertical. The IFS routines have been adapted to handle the retrieval profiles. In order to perform data assimilation experiments, screening and quality control procedures have been defined and implemented. This includes blacklisting, horizontal thinning of the data, model first guess check, and defining a realistic observation errors and error correlations. Further details of these quality control steps and choices will be discussed in the following sections.

4 Quality assessment

In this section the quality and characteristics of the retrievals are studied. This is done by comparing the temperature and humidity retrievals to their model counterparts. The diagnostic for the comparison is the observation minus model background (OmB) differences. The OmB differences can be used to characterise both systematic and random errors, and together with the quality and cloud information provided with the retrievals various investigations can be performed with the data. Overall, the quality of the retrievals is better and more homogeneous over sea than over land. Thus, in the following quality assessment the results are considered only for retrievals over sea as the aim is to select the best retrievals suitable for the first assimilation trials. It is also worth to note that the quality assessment has been done over two seasons, 1.1-31.3.2017 and 1.6-31.8.2017. The general conclusions from the two seasons are similar and the shown results cover the winter period only.

4.1 Using cloud and quality information in data selection

The cloud information provided with the retrievals is based on OmC values. I.e. the observed window channel brightness temperature is compared with the corresponding

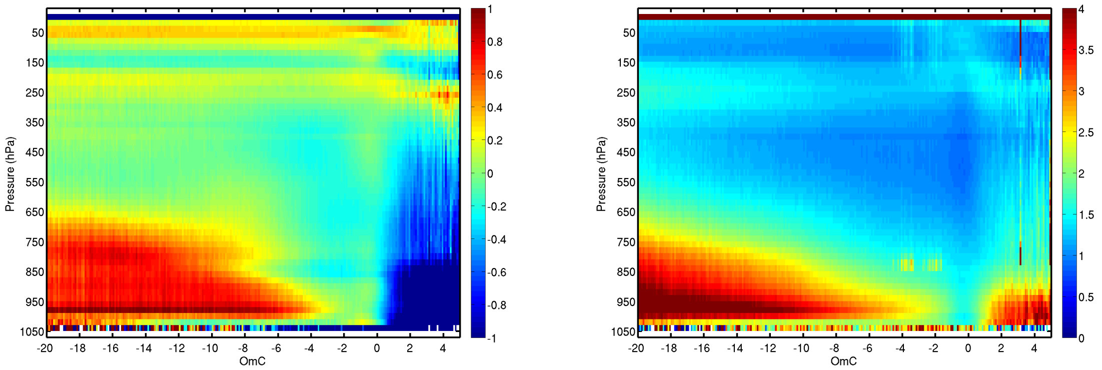

Figure 1: Observation minus background (OmB) bias (left panel) and standard deviation (right panel) for temperature with varying amount of cloud (OmC). Only profiles over sea are considered.

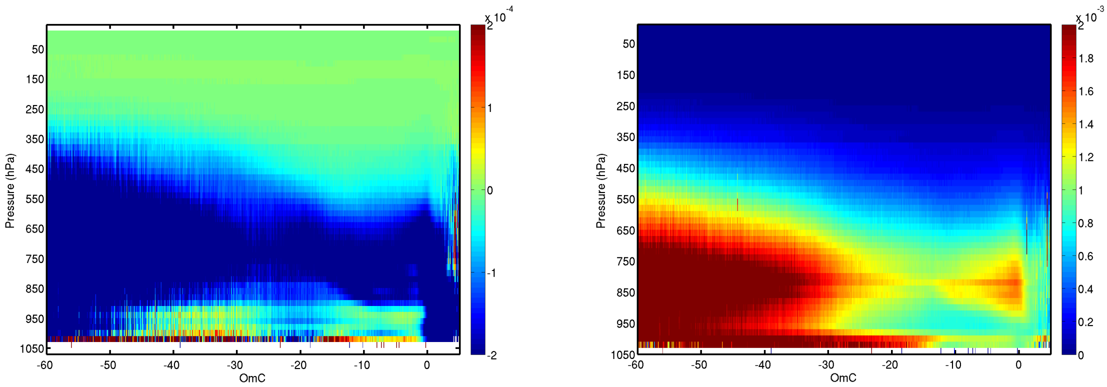

Figure 2: Same as Fig. 1 but for specific humidity.

brightness temperature calculated with a radiative transfer model making a clear sky assumption. Figure 1 shows the OmB bias (left panel) and standard deviation (right panel) for temperature for varying amount of cloud. It is clear that the clear sky temperature retrievals have the best quality both in terms of systematic and random errors, and the errors rapidly increase for cloud affected data. In this study retrievals with $|\text{OmC}| < 1$ are considered cloud free. This represents 11% of all available profiles.

Figure 2 shows the same as Fig. 1 but for specific humidity. The OmB statistics for humidity behave quite differently compared to the OmB statistics of temperature retrievals and the quality difference between the clear and cloud affected retrievals is not so obvious. Between 900 hPa and up to 300 hPa there is negative OmB bias, indicating that the model is on average more moist than the retrieval. According to Hultberg and August [20??] the negative bias for humidity originates from the sampling strategy used for the training data set in which the warmest instantaneous field of view in each effective field of view is chosen. The OmB standard deviation statistics indicate that the magnitude of random errors starts to increase significantly from OmC value -15 onwards.

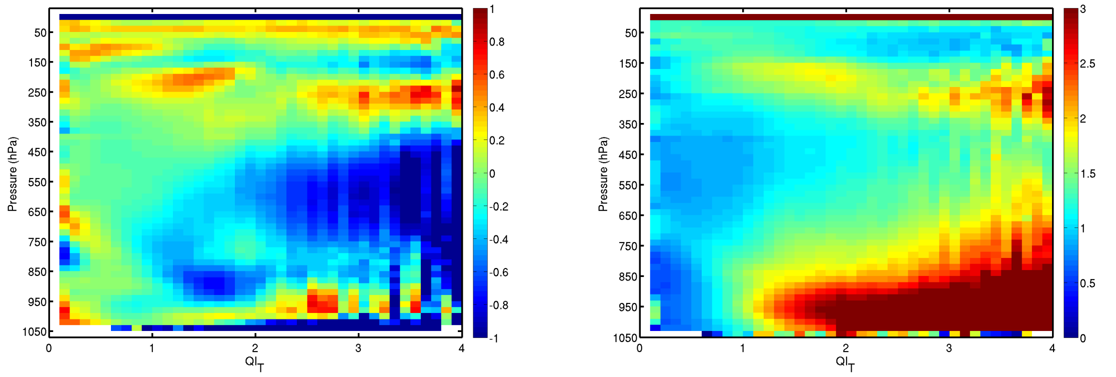

Figure 3: OmB bias (left panel) and standard deviation (right panel) for temperature retrievals with increasing QI_T.

The retrievals are complemented also with quality indicators. The most informative is the quality indicator for temperature (QI_T) which is an uncertainty estimate of the low tropospheric temperature. Figure 3 shows the OmB bias (left panel) and standard deviation (right panel) for temperature retrievals with increasing QI_T. Only data over sea is considered. Both OmB bias and standard deviation start to increase for QI_T values greater than 1. A criterion $QI_T < 1.5$ has been used in this study for the quality indicator. Applying this criterion on top of the cloud screening $|OmC| < 1$ results using 9% of the available profiles.

Right panel of Fig. 4 shows the OmB standard deviation profiles for the temperature retrievals. Blue line is indicating OmB standard deviation for all profiles over sea. Using the criterion $|OmC| < 1$ to select only clear sky profiles (red line) decreases the OmB standard deviation significantly, and using an additional criterion $QI_T < 1.5$ for the temperature quality indicator (black line) further decreases the OmB standard deviation especially below 500 hPa. The OmB standard deviation for high quality cloud free temperature retrievals is of the order of 1 - 1.5 K and for specific humidity less than $1.4 \cdot 10^{-3}$ Kg Kg^{-1} (not shown), depending on height. These statistics are similar or slightly larger in magnitude than similar statistics for radiosonde observations. The left panel of Fig. 4 shows the OmB bias profile for the temperature retrievals after the quality screening. There is a small negative bias below 400 hPa, indicating that the model profile is slightly warmer than the retrieval profile. This could be a signal of remaining cloud contamination.

Figure 4 indicates that above 30 hPa there is a strong negative bias in the temperature and the magnitude of random errors increases significantly as well. The quality assessment of the retrievals is done here against the IFS CY45R1. However, the training data set for the statistical retrievals has been taken from ERA5 based on IFS CY41R2 which was the operational cycle at ECMWF in 2016 [Hersbach et al., 2019]. The two IFS cycles have somewhat different temperature bias characteristics above 200 hPa, and increasingly in the stratosphere. Figure 5 shows the same as Fig. 4 (solid line) but in addition also

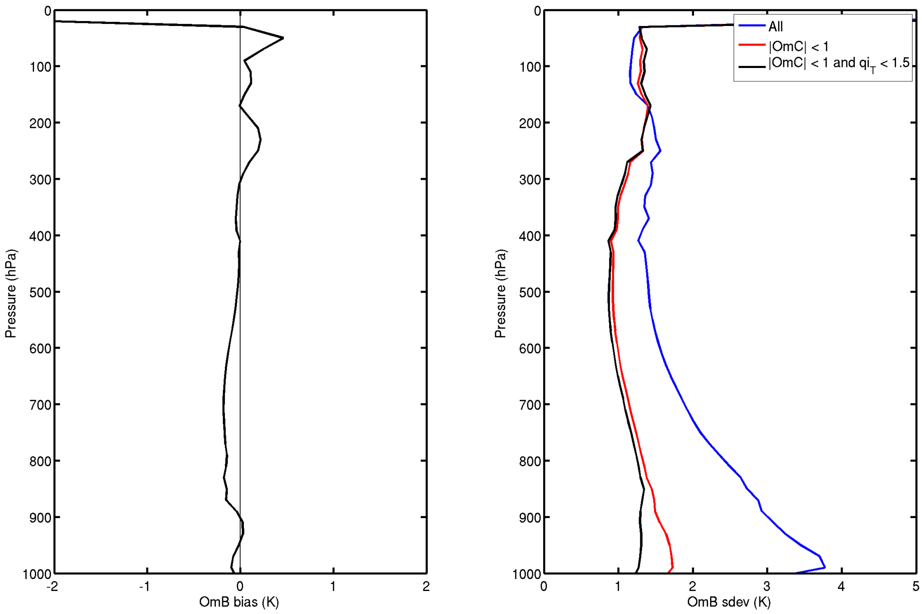

Figure 4: OmB bias (left panel) and standard deviation (right panel) profiles for temperature retrievals. Blue line indicates all profiles over sea, red line clear sky profiles selected with criterion $|\mathrm{OmC}| < 1$, and black line using additional criterion $\mathrm{QI_T} < 1.5$.

the OmB statistics calculated against ERA5 (dashed line) for the clear sky temperature retrievals. Below 200 hPa the statistics are nearly independent of the used model version but in the stratosphere and especially above 30 hPa the differences are large and quality assessment against ERA5 is not indicating the bias or significant increase in the magnitude of random errors. A feature of the statistical retrievals is that if the training base is biased with respect to the truth, the statistical method trained with that training base will inherit the same bias (reference MTG-IRS document, is this publicly available). Naturally, the aim is not to assimilate bias characteristics from an old model cycle. Thus, in the assimilation experiments performed in this study no retrieval information above 30 hPa is considered.

4.2 Fine scale vertical structures

General quality assessment of the retrievals indicates that the overall quality is quite good as long as strict quality criteria is applied to exclude cloudy scenes and an additional screening is done with the temperature quality indicator provided with the data. However, the retrievals are generally rather smooth and typically lack fine vertical structures, for example during low level temperature inversions and around the tropopause. These aspects are considered in more details in the following.

Table 1 summarises statistics how often a temperature inversion is captured in the model or in the retrieval profile during a three-month perion, 1.1-31.3.2017. The statistics

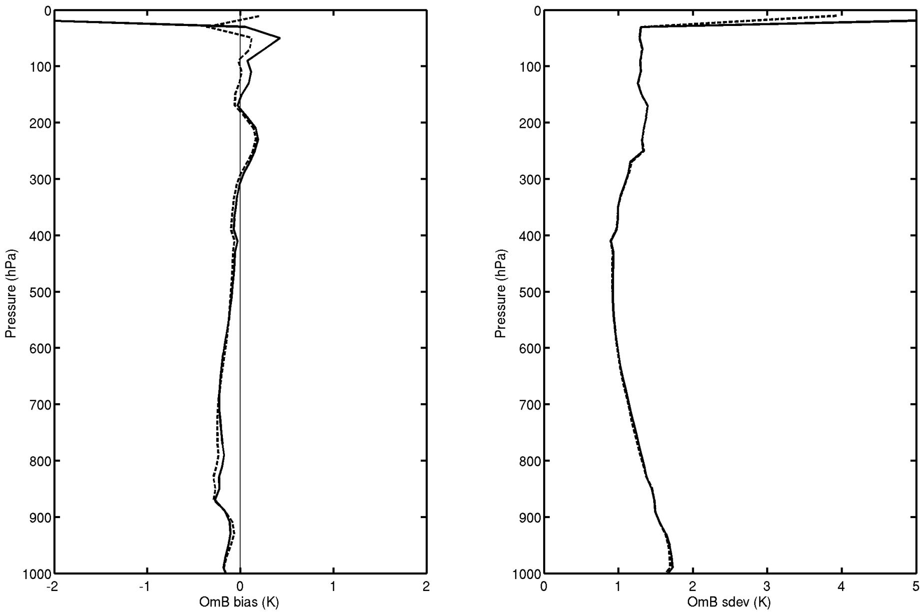

Figure 5: OmB bias (left panel) and standard deviation (right panel) profiles for temperature retrievals. Solid line indicates clear sky retrieval profiles compared against IFS CY45R1 and dashed line compared against ERA5 which is based on IFS CY41R2.

are calculated over the meteosat 0° geodisc area, separating midlatitudes and tropics. The model captures inversion in 65-68% of the profiles while the retrieval profiles in less than 20%. Understanding is that in reality temperature inversions occur even more frequently than in the model profiles. Thus, the statistics indicate that the retrievals are strongly underestimating the occurence of low level inversions.

Figure 6 compares the cases where temperature inversion is present in both profiles and reveals that in the retrievals the inversion is generally found from higher altitude than in the model profiles. The distribution of the model inversion heights in Fig. 6 represents very well also the general distribution of the inversion heights in the model.

Another challenge for the temperature retrievals is to capture details of the vertical

Table 1: Statistics how often a temperature inversion is present in the model or in the retrieval profiles. The statistics are calculated over the meteosat 0° geodisc area, separating northern and southern hemisphere midlatitudes and tropics. The covered period is 1.1-31.3.2017.

	Model: % of low level inversions	**Retrieval: % of low level inversions**
NH	64.6	10.8
TR	67.3	17.6
SH	67.6	19.4

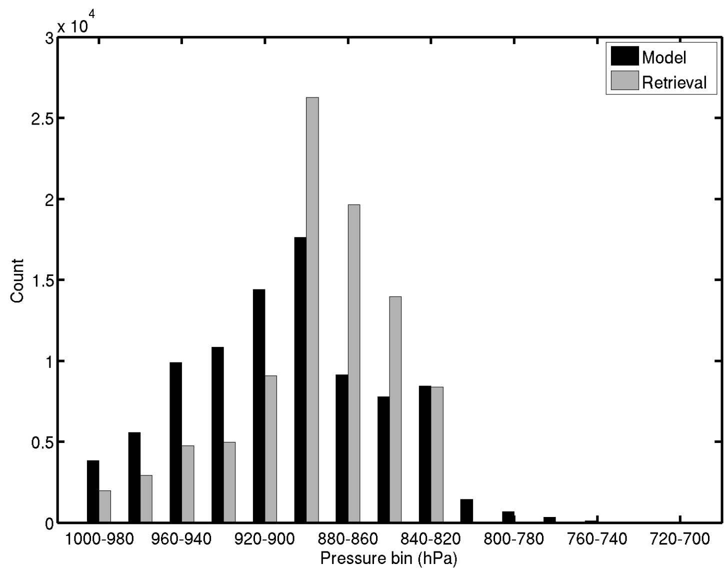

Figure 6: Distribution of the temperature inversion heights in the model profile (black) and in the retrieval profile (grey).

structures of the tropopause. Figure 7 shows a scatter plot of model tropopause temperatures in comparison to the retrieval tropopause temperatures in northern hemisphere midlatitudes. The colour scale indicates the latitude of the profile, blue shades being close to tropics and red shades representing higher latitudes. There is a set of cases where the agreement with the model and retrieval tropopause temperature is very good. However, in the second set the model tropopause is warmer, in extreme cases even 60 K, warmer. These cases originate mainly from relatively near the tropics. In these regions it is typical that there is a double tropopause structure, i.e. colder tropical tropopause is above the warmer polar tropopause and the retrieval profile is capturing only the cold higher tropical tropopause causing the large OmB difference in the tropopause temperature.

Thus, despite the quality assessment indicates that the overall quality of the clear sky retrievals is good and the OmB statistics suggest random errors roughly similar in magnitude than for radiosonde observations, it is important to recognise the smoothness of the retrieval profiles and take this into account in assimilation trials. One possibility would be to use averaging kernels which characterize the vertical sensitivity and resolution of the retrievals. In this study averaging kernels were not available and an attempt to take into account the smoothness of the profiles has been done by designing realistic observation errors and full error correlation matrix, as discussed in the following section 5.

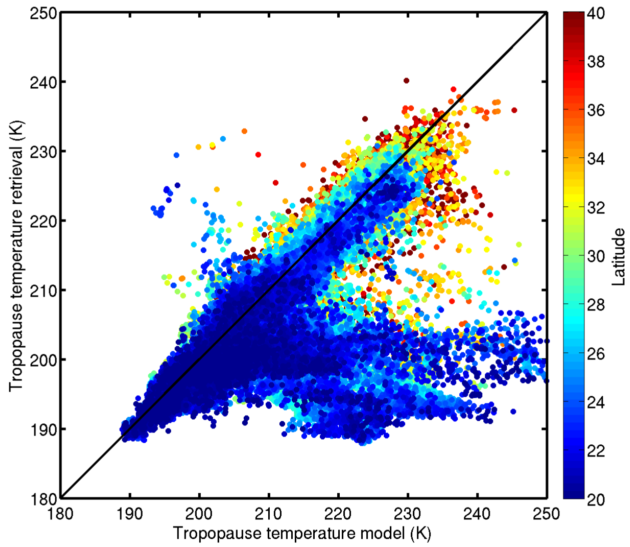

Figure 7: Scatter plot of model and retrieval tropopause temperatures. The colorscale indicates latitude of the profile.

5 Diagnosing the observation errors and error correlations in clear sky conditions

Specification of observation errors is an essential step for successful assimilation of any observation type. The assigned observation errors together with the specified background errors determine how much weight is given to the observations in the assimilation system. The observation error has two components, the representation error and the measurement error [Janjić et al., 2017]. The representation error consists of error due to unresolved scales and processes, observation operator error and pre-processing or quality control error. Measurement errors are such as instrument noise.

The observation errors and error correlations for the retrievals have been diagnosed following similar approach than what have been used for IASI radiances used in operations [Bormann et al., 2016]. First the Hollingsworth and Lönnberg [1986] method is used to obtain an initial estimate of the observation errors and vertical error correlations. Hollingsworth and Lönnberg [1986] method makes a strict assumption that observation errors are spatially uncorrelated and all spatial error correlations are due to background error. This assumption is relaxed in the second step in which the diagnosed errors and correlations are used in a new assimilation experiment, and the Desroziers et al. [2005] technique is applied to re-estimate the errors. When applying the Desroziers diagnostic, an assumption is made that the weights specified in the assimilation system are consistent with the true weights, introducing a potential dependence on the assumed background error. Experimentation has indicated that the sensitivity to the specification of the background error is relatively small [Bormann et al., 2015]. Finally the observation errors

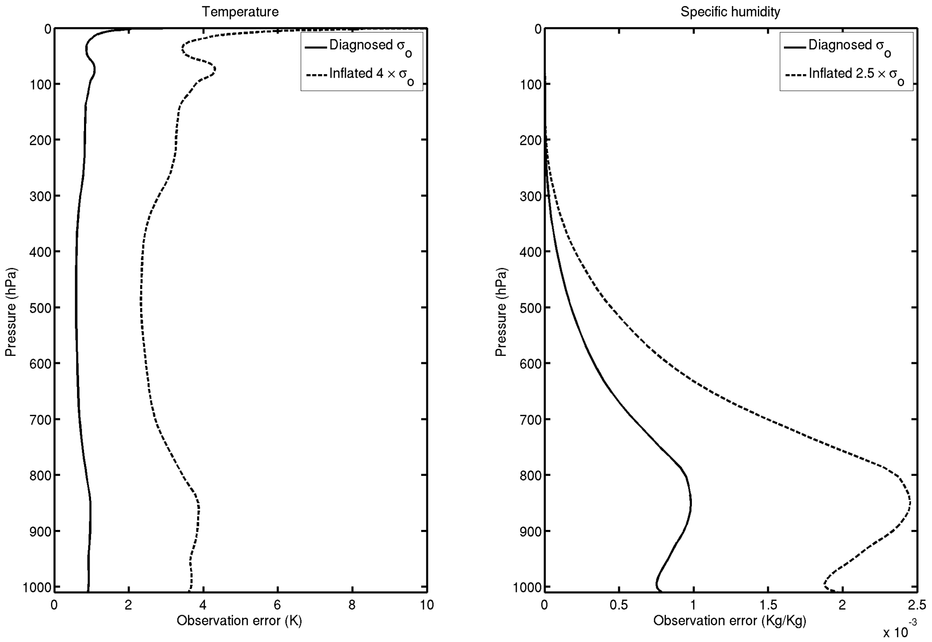

Figure 8: Observation errors for temperature (left panel) and specific humidity (right panel). Solid line indicates the errors diagnosed with the Desrozier technique and the dashed line indicates the inflated observation errors. Inflation factor of 4 is used for temperature and 2.5 for specific humidity errors.

are tuned by trial and error experimentation.

The retrieval errors have been diagnosed from experiments covering January 2017. Only clear sky profiles with criterion $|\mathrm{OmC}| < 1$ and $\mathrm{QI_T} < 1.5$ over sea are considered. Figure 8 shows the observation errors for temperature (left panel) and specific humidity (right panel) with solid line diagnosed with the Desroziers et al. [2005] technique. The diagnosed observation errors are relatively low in magnitude. Assimilation experiments indicate that inflating the errors, i.e. giving less weight to the retrievals than the diagnosed errors suggest, is beneficial for the analysis and forecast impact. Several inflation factors have been tested and it can be concluded that the errors for temperature require significant inflation. An inflation factor of 4 is used in the assimilation experiments discussed in the following. For humidity more moderate inflation of the errors is sufficient, and an inflation factor of 2.5 is applied in the assimilation experiments. The inflated observation errors are shown in Fig. 8 with dashed line. For temperature increase in the magnitude of the observation error is particularly evident around the typical altitudes of low level inversions and tropopause. Using large observation errors at these altitudes helps the model to retain the finer vertical structures that it has in the background field.

Figure 9 shows the vertical observation error correlations for temperature (left panel) and specific humidity (right panel). The error correlation matrices have been reconditioned with the eigenvalue method to make them numerically more stable [Bormann et al., 2015]. The retrievals have strong vertical error correlations, especially in the lower

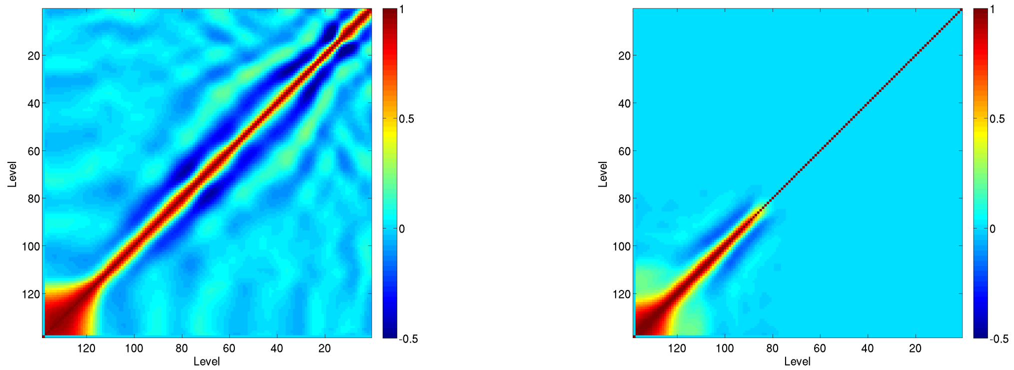

Figure 9: Vertical observation error correlations for temperature (left panel) and specific humidity (right panel) retrievals.

troposphere. Experimentation demonstrates that it is crucial to take these error correlations into account in the assimilation, in particular for the temperature retrievals as using the error correlations restricts how much the information of the missing or smooth vertical structures spreads in vertical in the analysis increments. This is illustrated with the next single observation experiment.

The temperature retrieval profile for the single observation experiment has been selected based on the fact that the provided quality information indicates that it is a high quality clear sky retrieval profile over sea with OmC value 0.36 and QI_T value 0.75. In addition, an important selection criterion has been that the IFS cloud detection system classifies all IASI channels cloud free for the corresponding radiance profile. Figure 10 shows the selected temperature retrieval profile (solid line) and the model background profile (dashed line), 1st January 2017 12.38 UTC, 39.26°N 33.41° W. Compared to the model background profile, the retrieval profile is missing the low level inversion and it has smoother tropopause structure.

First, the retrieval profile is assimilated with realistic observation errors (Fig. 8) but without taking into account the vertical observation error correlations. The resulting analysis increment profile is shown in the left panel of Fig.11 with solid line. Assimilating the temperature retrieval profile warms the analysis below 800 hPa and cools the analysis between 600 and 800 hPa, i.e assimilation of the retrieval profile makes adjustments to the model profile towards the missing inversion structure and the information is spread widely in vertical. For comparison, the analysis increment profile resulting from the assimilation of the corresponding IASI radiance profile is shown with dashed line in Fig. 11. Below 600 hPa the adjustments made to the model profile are opposite to the adjustments made by assimilation of the retrieval profile and are actually making the low level inversion sharper. The right panel of Fig. 11 shows the analysis inceremnt profile (solid line) when the temperature retrieval profile is assimilated using the full error correlation (Fig. 9). When the observation error correlations are taken into account, above 700 hPa assimilation of the retrieval profile brings more similar information into the system than assimilation

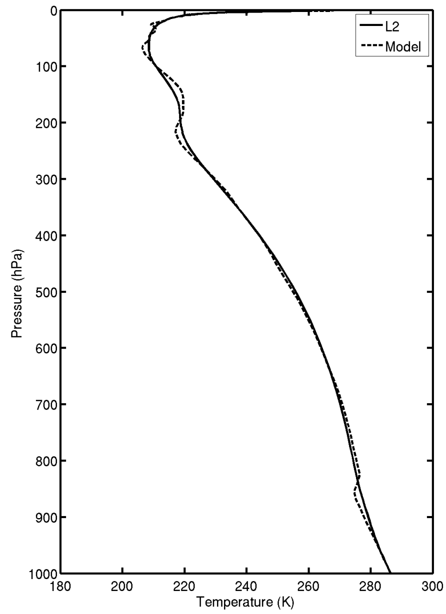

Figure 10: Temperature retrieval profile (solid line) and the model background profile (dashed line) used in the single observation experiment, 1st January 2017 12.38 UTC, 39.26°N 33.41°W.

of the radiance profile (dashed line). However, the signal is weaker due to the quite significant inflation of the observation errors and the strongest signal is still originating from the missing temperature inversion even though the signal is nor spread so much vertically compared to using a diagonal observation error correlation matrix.

6 Impact assessment of the clear sky retrievals

To investigate the impact of temperature and humidity retrievals on model analysis and forecasts, experiments with a depleted and with a full observing system have been performed with IFS cycle 45R1. The following subsections summarise the data selection procedures and the main results from the assimilation experiments in clear sky situations. The results are compared to the impact of assimilating the IASI radiances.

6.1 Data selection

The quality control and data selection consists of three steps. First, a so-called blacklist process rejects observations according to predefined rules. For the retrievals the following rules have been defined:

1. Clear sky profiles are selected with a criterion $|\mathrm{OmC}| < 1$. Quality assessment of the temperature retrievals has indicated that the errors increase rapidly for cloud

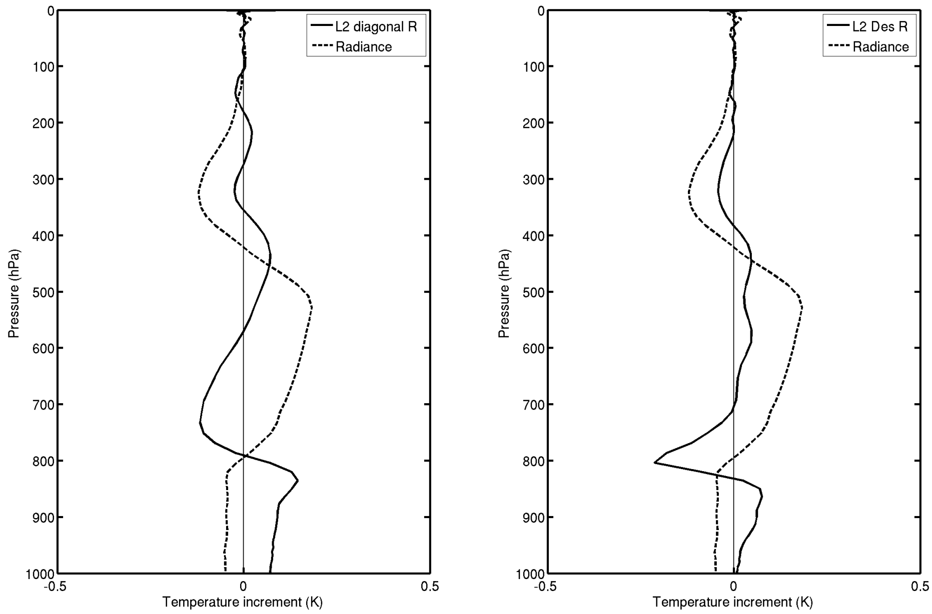

Figure 11: Temperature retrieval profile (solid line) and the model background profile (dashed line) used in the single observation experiment, 1st January 2017 12.38 UTC, 39.26°N 33.41°W.

affected profiles. Thus, at this stage they are excluded from the assimilation experiments. 11% of the profiles are considered cloud free with this criterion.

2. Only data over sea is used actively. This criterion ensures more homogeneous data quality and using global static observation errors and error correlations is a reasonable assumption.

3. A threshold $\mathrm{QI_T} < 1.5$ is applied for the temperature quality indicator provided with the retrievals. The quality indicator is an uncertainty estimate of the low tropospheric temperature. The applied criterion reduces the magnitude of the OmB standard deviation at low levels. Applying criterion for $\mathrm{QI_T}$ on top of rule 1 results using 9% of the available profiles.

4. No data above 30 hPa is used due to large temperature biases in the retrievals. The bias is inherited from ERA5 which is used as a training data for the statistical retrievals.

The second quality control step is the model first guess check. The first guess check compares observations y with the model background Hx_b

$$\frac{(Hx_b - y)^2}{\sigma_b^2 + \sigma_o^2} \leq L. \tag{1}$$

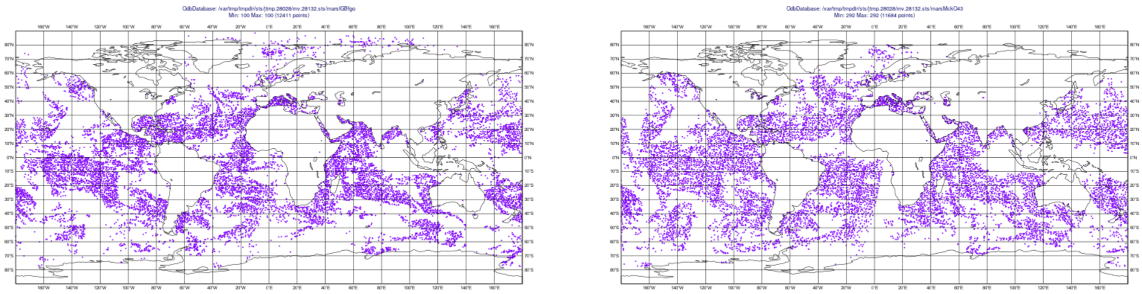

Figure 12: Sample coverage of active humidity retrievals (left panel) and IASI radiances (channel 3049, right panel) on 1st January 2017 00 UTC cycle.

Observations which deviate from the background more than a pre-defined limit L are rejected. In eq. 1 σ_b and σ_o are the background and observation errors, respectively. For the retrievals L is set to 9 which is a standard threshold used also for other temperature and humidity observations in the IFS system. Thus, the first guess check allows first guess departures which are maximum three times the expected error. The expected error is the square root of the sum of the squares of background error and observation error.

In addition of the performed quality control, the retrievals are thinned to 125 km resolution in horizontal. This is the same thinning distance than what is used for IASI radiances. The thinning is done to avoid horizontal observation error correlations which are not taken into account. Figure 12 shows a 12-hour sample coverage for the active humidity retrievals (left panel) and IASI radiances (right panel) for 1st January 2017 00 UTC cycle. There are ca 12740 active humidity profiles compared to ca. 11700 active IASI radiance profiles. The overall impression is that the number of active data is rather similar and the OmC based cloud detection for the retrievals is acting roughly in the same areas as the McNally and Watts [2003] cloud detection for the IASI radiances.

6.2 Assimilation experiments

Assimilation experiments have been performed both in depleted and in full observing system frameworks. Depleted observing system experimentation is a common methodology used to emphasise the impact of adding a single instrument or channel into the assimilation system. In a depleted observing system any changes can be attributed directly to the new added observations. Full observing system experimentation, on the other hand, gives a realistic understanding of the potential of the new observation type in a high quality state of the art operational system. Experiments have been run over a winter and summer season and the results are consistent with each other. In the following results covering the winter period are considered.

The following depleted system experiments have been run over a 2-month period, 1st

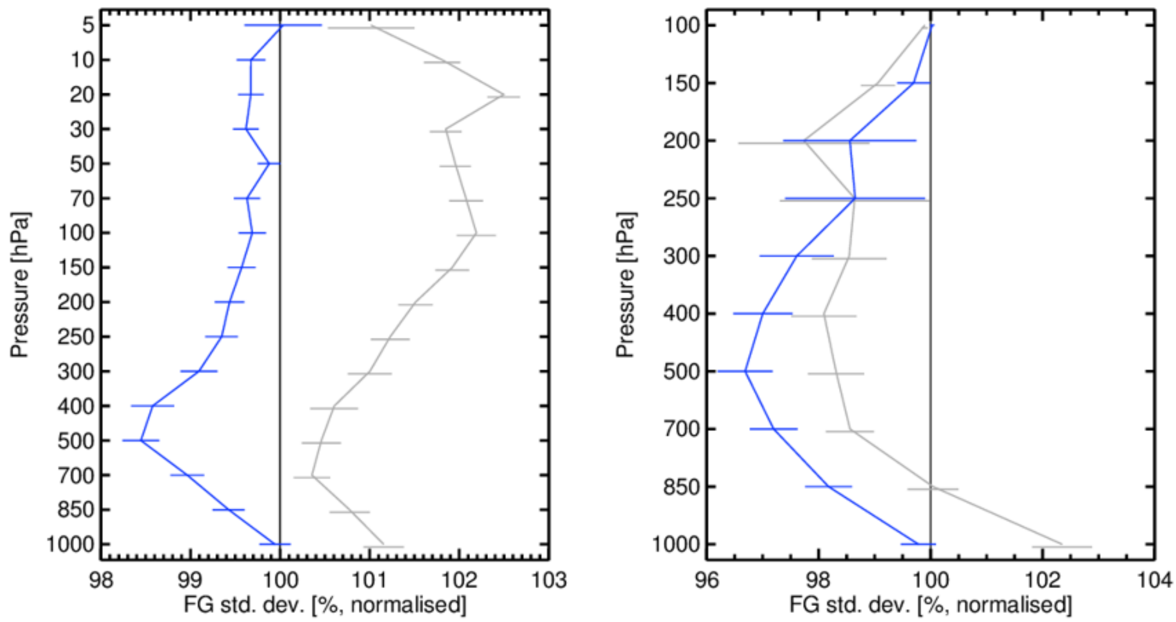

Figure 13: First guess departure standard deviation normalised by the depleted observing system baseline experiment for radiosonde temperature (left panel) and humidity (right panel) observations. The considered period is 1st January - 28th February 2017.

January - 28th February 2017.

- **Baseline**: conventional observations + AMSU-A
- **L2**: Baseline + temperature and humidity retrievals
- **IASI**: Baseline + IASI radiance observations used as in operations (over sea only)

The impact on short range forecasts is investigated by comparing the fit of the forecasts to independent observations. Figure 13 shows the first guess departure standard deviations normalised by the Baseline experiment for radiosonde temperature (left panel) and humidity (right panel). The grey line indicates the L2 experiment and the blue line the IASI experiment. Statistics below 100% indicate forecast improvement while values above 100% indicate degradation compared to the baseline experiment. Assimilation of the IASI radiances on top of the Baseline experiment results to clear statistically significant positive impact for short range temperature and humidity forecasts. In comparison, assimilation of the temperature and humidity retrievals indicates clear negative impact on temperature. The degradation is most likely due to assimilating the smooth or missing vertical structures for temperature without taking the limited vertical resolution of the retrievals properly into account when using a global average of the observation errors and static error correlation. The impact on humidity is positive and assimilation of the retrievals is able to bring rather similar positive impact into the system than assimilation of the radiances.

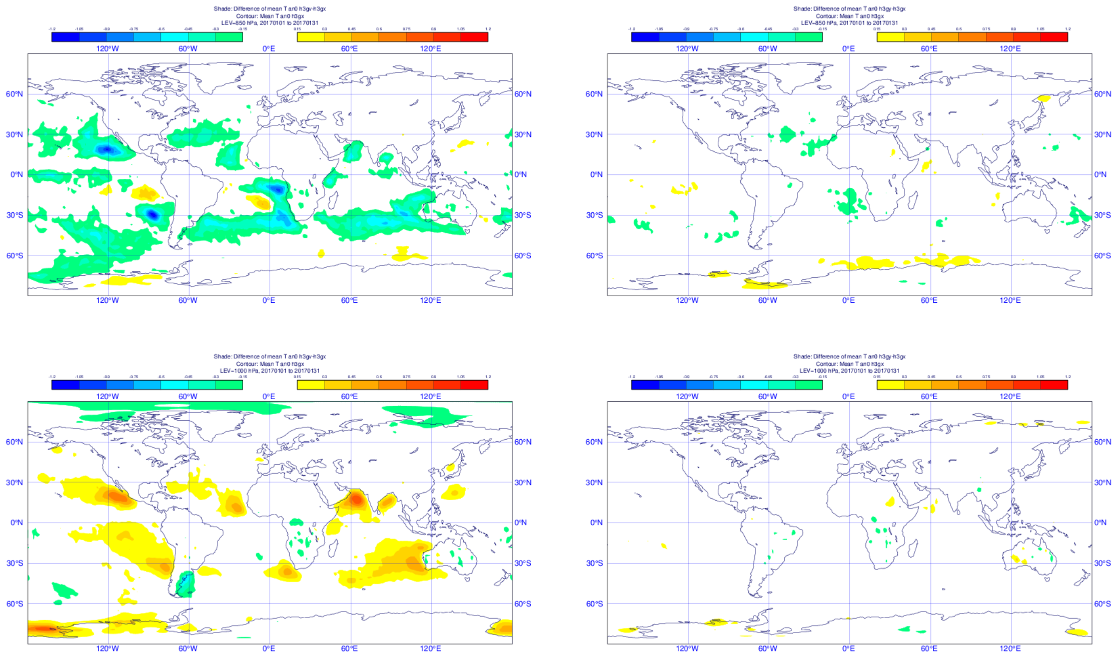

Figure 14: Mean analysis difference between the L2 and Baseline experiments (left panels) and between IASI and Baseline experiments (right panels) for temperature at 850 hPa (upper panels) and 1000 hPa (lower panels) levels calculated over January 2017. Experiments have been run in full observing system.

In the full observing system experiments the **Baseline** is using all operationally used observations except IASI radiances. Similar to the depleted observing system experiments, either temperature and humidity retrievals or IASI radiances are added on top of the baseline experiment.

Figure 14 shows the mean analysis difference between the L2 and Baseline experiments (left panels) and between IASI and Baseline experiments (right panels) for temperature at 850 hPa (upper panels) and 1000 hPa (lower panels) levels calculated over January 2017. Overall, assimilation of the retrievals in the full observing system is making significantly stronger adjustments to the temperature analysis fields than assimilation of IASI radiances. In case of the retrieval assimilation, the mean analysis difference fields indicte that the largest differences are found in subtropical regions in the eastern parts of oceans, which are typically associated with persistent marine stratus and characterized by sharp inversions at the top of the bloudary layer [Muhlbauer et al., 2014]. Thus, the results indicate that the model is making adujstments to the analyses to better fit the retrieval profiles lacking the low level inversions.

Figure 15 shows the first guess departure standard deviations normalised by the baseline experiment for radiosonde temperature (left panel) and humidity (right panel) for the full observing system experiments. The results are consistent with the depleted observing system, indicating negative impact for temperature and positive impact, again very similar of IASI radiances, on humidity from the assimilation of the retrievals.

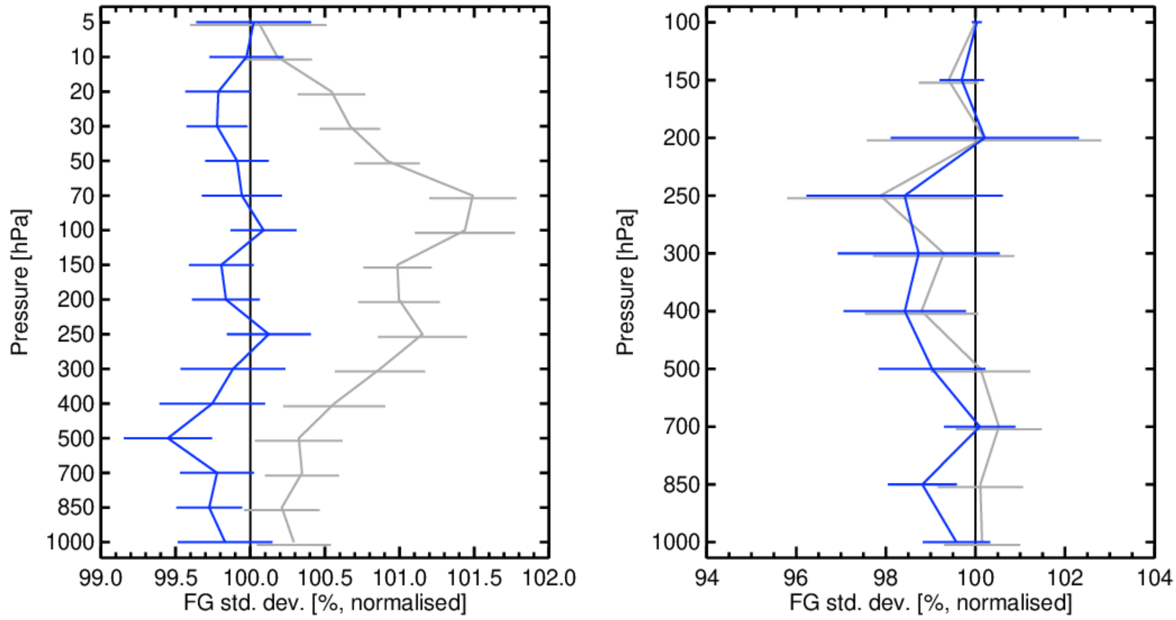

Figure 15: Same as Fig. 13 but for the full observing system experiments.

7 Impact assessment of the cloud affected humidity retrievals

Experiments in clear sky conditions indicate positive impact from assimilation of the humidity retrievals. In this section the focus is on investigating the potential of using cloud affected humidity retrievals to further improve the analysis and forecasts. The temperature retrievals are excluded from the experimentation. Again the experiments have been done in depleted and in full observing system framework. The results are consistent in both experiment setups and in the following only results from the depleted observing system experiments are shown. IASI radiances are used only in clear sky scenes, thus comparison to assimilation of cloud affected radiances is not done at this stage.

7.1 Use of clear sky observation errors and error correlations

First, the potential of assimilating cloud affected humidity retrievals using observation errors and error correlations derived for the clear sky situations is investigated. The experiments introduce gradually increasing amount of cloud affected humidity retrievals into the system:

- **EXP1**: -1 $<$ OmC $<$ 1
- **EXP2**: -5 $<$ OmC $<$ 1
- **EXP3**: -15 $<$ OmC $<$ 1

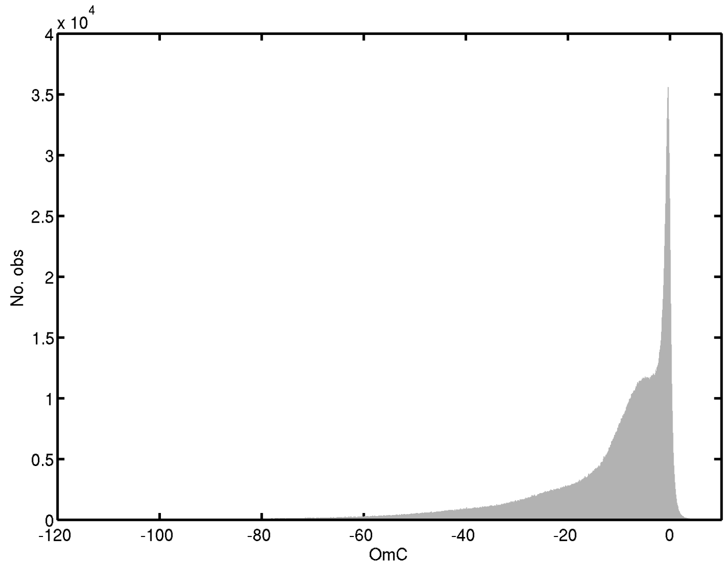

Figure 16: Distrubution of observations for different OmC values.

- **EXP4**: -30 < OmC < 1
- **EXP5**: -45 < OmC < 1
- **EXP6**: -60 < OmC < 1

Figure 16 shows the distrubution of observations for different OmC values. **EXP1** is assimilating clear sky humidity profiles only, and using 9% of the available data while **EXP6** is using 98% of the available humidity profiles and includes also the most cloud affected profiles.

In these experiments the observation errors and error correlation derived for clear sky situations are used. As discussed in Section 4 and Fig. 2, the increase in the OmB standard deviation starts from OmC -15 and onwards, i.e. the behaviour is rather different than for temperature. As the clear sky observation errors diagnosed with the Desroziers method are inflated by a factor of 2.5 it can be expected that these errors are a reasonable first estimate of the observation errors for cloud affected situations as well.

Figure 17 shows the normalised first guess departure standard deviation for **EXP1** and **EXP6**. It is worth to note that when only humidity retrieval profiles are assimilated in the clear sky conditions (**EXP1**) the impact on short range temperature forecasts is neutral. Introducing cloud affected retrievals into the system brings further benefits to the short range humidity forecasts with no sign of saturation in the impact even for the most cloud affected cases. However, for OmC < -15 and smaller the temperature forecasts starts to degrade. The results in the full observing system experiments are consistent with the depleted observing system experiments (not shown).

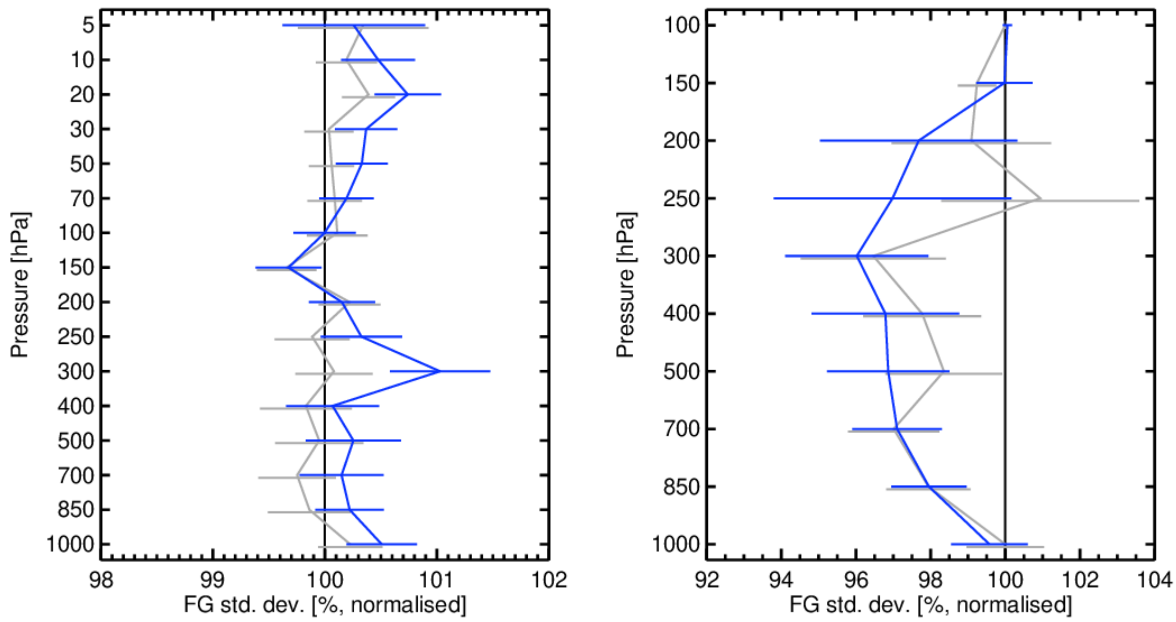

Figure 17: First guess departure standard deviation normalised by the depleted observing system baseline experiment for radiosonde temperature (left panel) and humidity (right panel) observations. The considered period is 1st January - 28th February 2017. **EXP1** is shown with grey line and **EXP6** with blue line.

7.2 Use of scene dependent observation errors

The interesting question is of course, if the impact of the cloud affected humidity retreivals can be further enhanced by taking into account scene dependent observation errors. Figure 18 show the OmB standard deviation at 300 hPa (left panel) and 900 hPa (right panel) levels for different OmC values as snapshots from Fig. 2. The increase in the OmB standard deviation is quite linear for OmC values -15 and smaller.

As a first approach to take into account the scene dependence, a generalised observation error model has been developed and used at all altitudes. Figure 19 illustrates the behaviour of the observation error model. The clear sky observation errors are used for humidity profiles with $-15 < \mathrm{OmC} < 1$. For $\mathrm{OmC} < -15$ the clear sky observation error is linearly increased so that for $\mathrm{OmC} = -60$ the used observation error is three times the clear sky error value.

The scene dependent observation error model has been tested in an experiment using criterion $-60 < \mathrm{OmC} < 1$ for data selection. Figure 20 shows the normalised first guess departure standard deviation for temperature (left panel) and humidity (right panel). The positive impact on humidity remains very similar as in case of using the clear sky observation errors. However, the degradation seen in temperature forecasts is either removed (depleted observing system) or significanly decreased (full observing system, not shown).

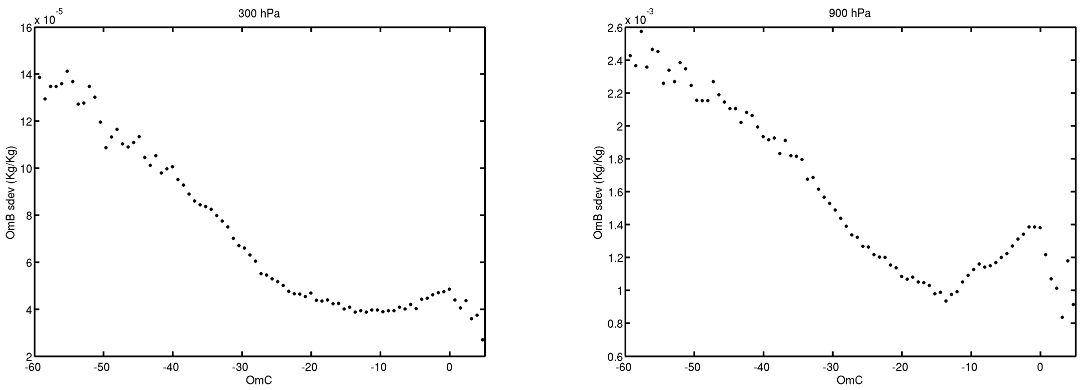

Figure 18: OmB standard deviation at 300 and 900 hPa levels for different OmC values as snapshots from Fig. 2

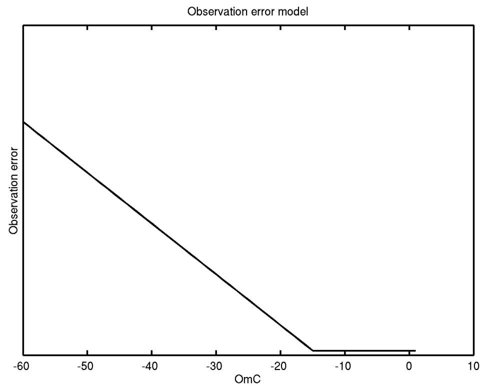

Figure 19: Behaviour of the observation error model.

7.3 Use of scene dependent observation error correlations

A further refinement for assimilation of cloud affected humidity retrievals is to take into account the increased affect from cloud in the observation error correlations. Figure 21 shows examples of observation error correlations for specific humiduty, diagnosed with the Desroziers method, with OmC values -1 $<$ OmC $<$ 1, -10 $<$ OmC $<$ -2, -30 $<$ OmC $<$ -15 and -60 $<$ OmC $<$ -45. It is obvious that with increasing impact of cloud in the retrieval field of view, the observation error correlations become stronger and using the clear sky error correlations significantly underestimates them in assimilation experiments.

One possibility to inflate the error correlation matrix is to inflate the leading eigenvalue of the matrix. This has been tested as a first approach for scene dependent observation error correlations. The procedure is the following. First an eigenvalue decomposition is done for the error correlation matrix. The leading eigenvalue λ is modified to be λ^{γ} where γ is the inflation factor. The behaviour of γ with OmC is illustrated in Fig. 22. The error correlation matrix is then reconstructed and used as a scene depenent error covariance together with the scene dependent observation errors. Figure 22 shows also

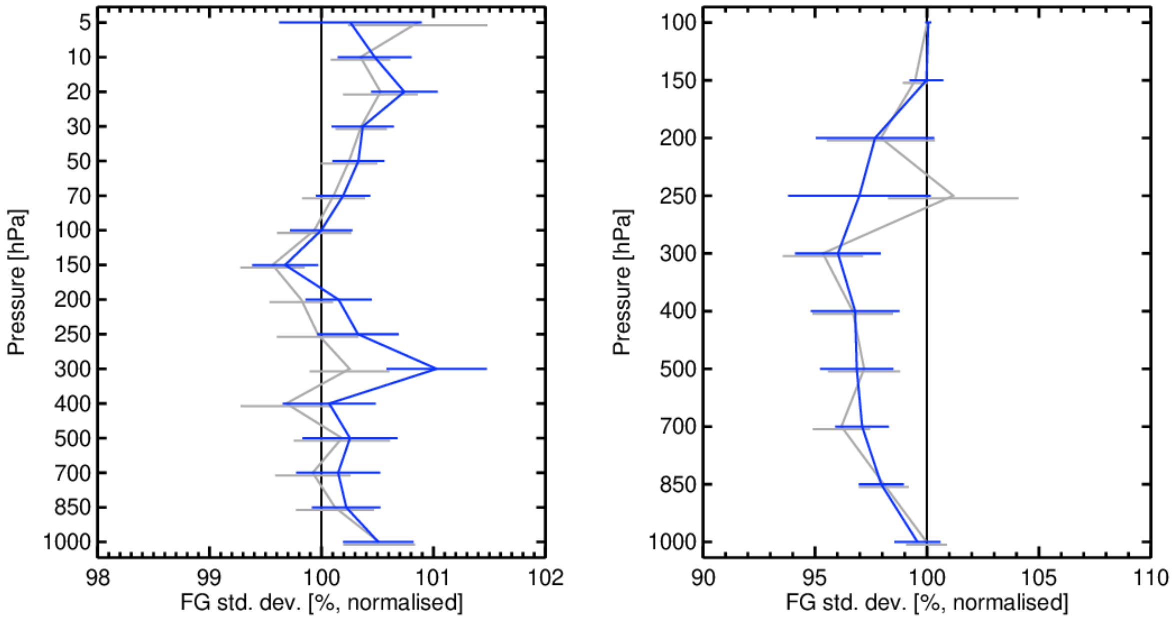

Figure 20: Same as Fig. 17 but for **EXP6** (blue line) and experiment using the observation error model (grey line).

examples of the inflated error correlation with OmC values -10, -30 and -60.

The impact of using the scene dependent observation errors and correlations is illustrated in Fig. 23. This time the control experiment, i.e. 100% line, is experiment using the cloud affected humidity retrievals with observation errors and correlation diagnosed for clear sky scenes. Grey line indicates the experiment using both scene dependent observation errors and correlations, while the blue line indicates experiment using the scene dependent observation errors but static clear sky error correlation. Impact of taking into account the scene dependence in the observation error and correlations is clearly beneficial.

8 Feasibility of importing level 2 observation errors

One extremely relevant question in using the retrievals is the data volume distributed. In this study, retrievals in the IASI native grid are considered. This means that for each pixel there is temperature, humidity and ozone profile on 137 vertical levels, surface information and additional quality information. This results to similar data amounts than what are operationally monitored for IASI radiances in the ECMWF system. A pre-screening step to select one out of four pixels is applied for the radiances and similar approach was adapted for the retrievals as well to make the data handling more practical. Data is further thinned inside IFS to avoid horisontal error correlations which are not taken into account in the assimilation. The retrievals used in this study are accompanied with cloud and quality information, one value for each profile. Thus, no error estimates for

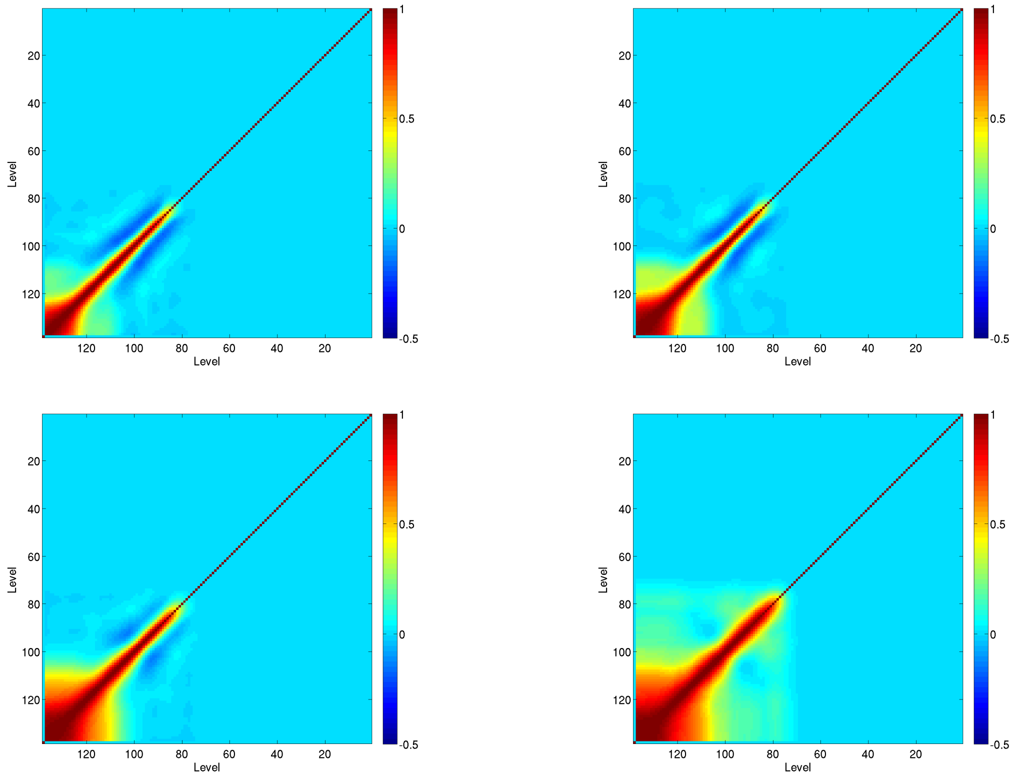

Figure 21: Observation error correlations for specific humiduty, diagnosed with the Desroziers method, with OmC values -1 < OmC < 1 (upper left panel), -10 < OmC < -2 (upper right panel), -30 < OmC < -15 (lower left panel) and -60 < OmC < -45 (lower right panel).

different levels of the profile are provided. In this case the user diagnoses the observation errors and error correlations to be used in data assimilation. This requires extensive experimentation and is relatively time and resource consuming.

The most sophisticated way to use the retrievals would be to provide the retrievals in the native grid together with scene dependent averaging kernels, observation errors and/or error correlations for each individual profile. Averaging kernels communicate to the assimilation system the way in which the observing system smooths the profile. In an ideal inverse method the averaging kernel matrix would be a unit matrix but in reality the rows of the matrix are peaked functions, peaking at the appropriate level, and with a half-width which is a measure of the spatial resolution of the observing system [Rodgers, 2000]. Thus, averaging kernels provide a simple characterisation of the relationship between the retrieval and true state of the atmosphere. However, the approach to provide full error information and averaging kernels for each pixel is not practical as it leads to enourmous data volumes. Observation error profiles would be additional 3×137, error correlations $3 \times 137 \times 137$, and averaging kernels $3 \times 137 \times 137$ matrices for each pixel.

Two alternative ways could be considered to make the most sophisticated option lighter in the distributed data volume. It is known that the retrieval profile does not

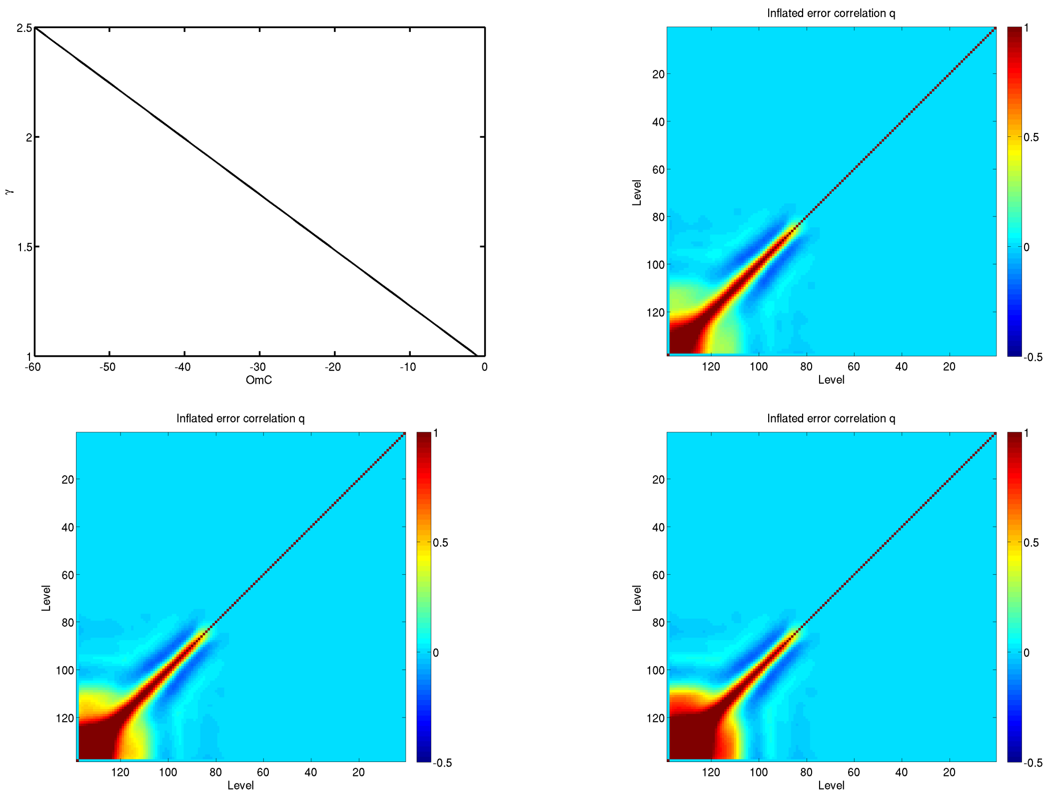

Figure 22: Inflation factor γ (upper left panel) and examples of the inflated error correlation matrix with OmC values -10 (upper right panel), -30 (lower left panel) and -60 (lower right panel).

include 137 independent pieces of data and its actual vertical resolution is much less. Thus, one alternative would be to dissminate retrievals in reduced grid/layering with full error profiles and correlations. For example distributing the retrievals on 15 levels, with the full error profile and correlations would result to similar data amounts than full MTG-IRS spectrum with 1900 channels for each pixel.

The other option, and currently under consideration at EUMETSAT, is to distribute the retrievals at all 137 levels together with surface and quality information and provide the scene dependent errors and averaging kernels as a separate data base from which the user selects the most appropriate error information and averaging kernel for each profile when using the data. This will keep the volume of the actively distributed data on the same level as it has been for the retrievals used in this study. A follow on phase of this project, starting February 2020, will focus on investigating the feasibility of the use of the retrievals with scene dependent averaging kernels provided by EUMETSAT.

9 Conclusions and outlook

The objectives of this study have been to evaluate the potential and practical aspects of assimilating the temperature and humidity profiles retrieved from IASI, as proxy for

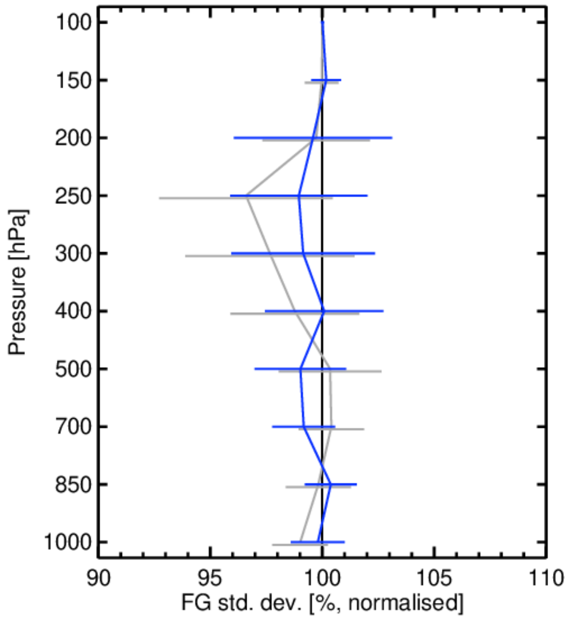

Figure 23: Same as Fig. 20 right panel but the control experiment (100% line) is experiment using the cloud affected humidity retrievals with observation errors and correlation diagnosed for clear sky scenes. Grey line indicates the experiment using both scene dependent observation errors and correlations, while the blue line indicates experiment using the scene dependent observation errors but static clear sky error correlation.

MTG-IRS L2 products, in the numerical weather prediction model of ECMWF. The all-sky retrieval function from the operational IASI L2 processor in the infrared-only mode has been used.

Comparison of the retrievals and their model counterparts indicate that the overall quality of the retrievals is good when strict quality control based on cloud and quality information provided with the retrievals is applied, especially for the temperature profiles. In clear sky situations the deviations between model background and the retrievals are roughly comparable in magnitude to similar statistics computed for radiosondes. However, the retrieval profiles are rather smooth due to the vertical resolution of the IASI instrument, and are often lacking vertical details of for example low level temperature inversions or fine scale tropopause structures. Investigations reveal that the observation errors are also highly correlated between vertical levels. It is essential to take these correlations into account in data assimilation experiments. The error correlations are situation and location dependent and become increasingly stronger for cloud affected profiles.

Assimilation experiments indicate that in clear sky conditions the humidity retrievals have a positive impact on analyses and forecast quality, comparable in magnitude to that obtained when IASI radiances are assimilated. Assimilation of cloud affected humidity retrievals brings further improvements to model analyses and forecasts. Impact can be enhanced by using scene dependent observation errors and error correlations that have been developed in this study. The experiments also show that the assimilation of temperature retrievals currently degrades the analysis and forecasting system. This is likely due to assimilation of the smooth or missing vertical structures for temperature without taking the limited vertical resolution of the retrievals properly into account through averaging kernels in the observation operator.

The follow on extension of the project will focus on investigating the practical and scientific potential of assimilating the proxy MTG-IRS temperature and humidity retrievals with their averaging kernels, as a characterization of their vertical sensitivity and resolution. This requires that the IFS assimilation framework is extended to include vertical resolution and sensitivity functions in the observation operator. The significance of the vertical uncertainty estimates for temperature and humidity will also be evaluated for quality control, with the aim to select the data for assimilation and possibly dynamically adapt the observation error.

References

E. Andersson, A. Hollingsworth, G. Kelly, P. Pailleux, and Z. Zhang. Global observing system experiments on operational statistical retrievals of satellite sounding data. *Mon. Wea. Rev.*, 119:1851–1865, 1991.

M. J. Atkins and M. Jones. An experiment to determine the value of SIRS data in numerical forecasting. *Meteorol. Mag.*, 104:125–142, 1975.

N. Bormann, M. Bonavita, R. Dragani, R. Eresmaa, M. Matricardi, and A. McNally. Enhancing the impact of IASI observations through an updated observation-error covariance matrix. *ECMWF Technical Memorandum*, 756, https://www.ecmwf.int/en/elibrary/8292-enhancing-impact-iasi-observations-through-updated-observation-error-covariance 2015.

N. Bormann, M. Bonavita, R. Dragani, R. Eresmaa, M. Matricardi, and A. McNally. Enhancing the impact of IASI observations through an updated observation-error covariance matrix. *Q. J. R. Meteorol. Soc.*, 142(697):1767–1780, 2016.

F. Bouttier and G. Kelly. Observing-system experiments in the ECMWF 4D-Var data assimilation system. *Q. J. R. Meteorol. Soc.*, 127:1469–1488, 2001.

G. Desroziers, L. Berre, B. Chapnik, and P. Poli. Diagnosis of observation, background and analysis-error statistics in observation space. *Q. J. R. Meteorol. Soc.*, 131:3385–3396, 2005.

EUMETSAT. IASI Level 2: Product guide. *Available at: https://www.eumetsat.int/website/home/Data/TechnicalDocuments/index.html*, 2017.

J. R. Eyre. Progress achieved on assimilation of satellite data in NWP. *ECMWF Seminar on Recent Development in the Used of satellite observations in NWP, Reading, United Kingdom, 3-7 September 2007*, 2007.

H. Hersbach, B. Bell, P. Berrisford, A. Horányi, J. Muõz Sabater, J. Nicolas, R. Radu, D. Schepers, A. Simmons, C. Soci, and D. Dee. Global reanalysis: goodbye ERA-Interim, hello ERA5. *ECMWF Newsletter*, 159:17–24, 2019.

A. Hollingsworth and P. Lönnberg. The statistical structure of short-range forecast errors as determined from radiosonde data. Part I: The wind field. *Tellus*, 38A:111–136, 1986.

T. Hultberg and T. August. The piecewise linear regression retrieval of temperature, humidity and ozone with the EUMETSAT IASI L2 PPF version 6. 20??

T. Janjić, N. Bormann, M. Bocquet, J. A. Carton, S. E. Cohn, S. L. Dance, S. N. Losa, N. K. Nichols, R. Potthast, J. A. Waller, and P. Weston. On the representation error in data assimilation. *Q. J. R. Meteorol. Soc.*, 144(713):1257–1278, 2017.

G. Kelly, E. Andersson, A. Hollingsworth, P. Lönnberg, P. Pailleux, and Z. Zhang. Quality control of operational physical retrievals of satellite sounding data. *Mon. Wea. Rev.*, 119:1866–1880, 1991.

G. A. Kelly and J. Pailleux. Use of satellite vertical sounder data in the ECMWF analysis system. *ECMWF tech. Memo*, 143, 1988.

G. A. M. Kelly, G. A. Mills, and W. L. Smith. Impact of nimbus-6 temperature soundings on australian regional forecasts. *Bull. Am. Meteorol. Soc.*, 59:393–406, 1978.

S. Lord, G. Gayno, and F. Yang. Analysis of an observing system experiment for the joint polar satellite system. *BAMS*, 97:1409–1425, 2016.

A. McNally and P. Watts. A cloud detection algorithm for high-spectral-resolution infrared sounders. *Q.J.R. Meteorol. Soc.*, 129:3411–3423, 2003.

A. McNally, M. Bonavita, and J.-N. Thépaut. The role of satellite data in the forecasting of hurricane Sandy. *Mon. Wea. Rev.*, 142:634–646, 2012.

A. Muhlbauer, I. L. McCoy, and R. Wood. Climatology of stratocumulus cloud morphologies: microphysical properties and radiative effects. *Atmos. Chem. Phys.*, 14: 6695–6716, 2014.

G. Ohring. Impact of satellite temperature sounding data on weather forecasts. *Bull. Am. Meteorol. Soc.*, 60:1142–1147, 1979.

C. D. Rodgers. Inverse methods for atmospheric sounding, Theory and Practice. *World Scientific, River Edge*, 240 pp, 2000.